Chemistry of Vibronic Coupling. 3. How One Might Maximize Off-Diagonal Dynamic Vibronic Coupling Constants for Intervalence Charge-Transfer (IVCT) States in an ABA• System (A, B = Alkali Metal, H, Halogen)?

Wojciech Grochala and Roald Hoffmann*

Department of Chemistry and Chemical Biology, Cornell University, Ithaca, New York 14853-1301

Received: May 12, 2000; In Final Form: August 3, 2000

We investigate computationally the vibronic coupling constant in a large group of simple uncharged ABA• systems (A, B = H, Li, Na, K, Rb, Cs, F, Cl, Br, I), which may be formally mixed-valence or intermediate-valence ones. These open-shell species belong to three chemically quite distinct groups: intermetallic, interhalogen, and salt-like triatomics. Constraining these systems to a linear symmetric geometry, we optimize the A−B bond length at a certain level of theory and determine the electronic and vibrational structure of such species. At this common geometry we calculate a vibronic stability parameter for the antisymmetric mode (*G*), defined as the *ratio* of force constants for the antisymmetric to the symmetric stretching mode. *G* is a sensitive indicator of the magnitude of vibronic coupling. Values of *G* smaller than 1 (asymmetric mode softening) indicate large values of the off-diagonal vibronic coupling constant. Negative *G* indicate very large values of that constant, leading to vibronic instability. The smallest values of *G* are obtained for interhalogen species (most of them are vibronically unstable). Salt-like ABA and BAB molecules, as well as intermetallic species are vibronically stable. Two further interesting correlations evolve: the calculated force constants for the symmetric stretching mode correlate well with *f*, a parameter defined as the sum of the electronegativities of the A and B elements divided by the AB bond length. Large values of *f* also indicate strong vibronic coupling.

Introduction

In the present paper we investigate theoretically the off-diagonal vibronic coupling constant (VCC)[1] for some simple ABA• molecular systems. Such systems may be formally mixed-valence (MV) or intermediate-valence (IV) ones. The MV systems are those where the two A atoms are not equivalent (the molecule is asymmetric in the ground state, the two AB bond lengths are different). The IV systems are those where two A atoms are equivalent. Historically, the fruitful division into MV and IV complexes took shape in another context after discovery of the well-known Creutz and Taube complex.[2] This led to a number of theories for MV complexes, the best known of these being Marcus-type theories using a harmonic potential model.[3]

The MV (asymmetric) systems exhibit a photon driven or thermally driven intervalence charge-transfer (IVCT) transition. An IVCT process in the solid state is also believed to influence the critical temperature (T_c) of cuprate high-temperature superconductors (HTSC).[4] Our aim in a series of contributions is to learn how to tune the dynamic VCC in different MV or IV molecules, similar to our exploration of the *diagonal* VCC for ligand-to-metal charge-transfer (LMCT) states.[5]

The thermal IVCT may (but does not necessarily have to) lead to a structure energetically *equivalent* with the starting one. An example is

$$Fe^{3+}-O^{2-}\cdots Fe^{2+} \rightleftarrows Fe^{2+}\cdots O^{2-}-Fe^{3+}$$

On the other hand, LMCT or metal-to-ligand charge-transfer (MLCT) usually generates strongly nonequivalent electronic state, with typically higher barriers separating minima. This is exemplified by

$$Fe^{3+}-O^{2-}\cdots Fe^{2+} \rightarrow Fe^{2+}\cdots O^{\bullet 1-}\cdots Fe^{2+}$$

Among the two CT processes discussed here, only thermal IVCT in the solid state (but not LMCT or MLCT) may give rise to free charge movement (electrical conductivity), and this only under certain circumstances. Free charge carriers may further condense into Cooper boson pairs, essential for superconductivity.[6] Thus, investigations of vibronic coupling (VC) connected with IVCT in superconducting materials are usually more common than those relevant to LMCT or MLCT.

We are especially interested in the relationship between values of the VCC and the chemical character of A and B atoms constituting an ABA molecule, i.e., in *trends* helping us in predicting qualitatively whether VCC increases or decreases upon a given chemical substitution. To put it in another way, we are in search of "the chemistry of the off-diagonal vibronic coupling constant for IVCT".

ABA molecules of the type Me_2X and MeX_2 (where Me = alkali metal, X = halogen) are very interesting per se. They are sometimes called superalkalis[7,8] and superhalogens,[9,10] respectively. This is because some of these molecules have ionization potentials which are actually smaller in magnitude than that of Cs metal. On the other hand, molecules with an electron affinity higher than that of the F atom exist in the second group. Experimental information for ABA molecules is often lacking in the literature, partially due to their high instability with respect to electron transfer.

* To whom correspondence should be addressed. E-mail: rh34@cornell.edu.

10.1021/jp0017745 CCC: $19.00
Published on Web 10/10/2000

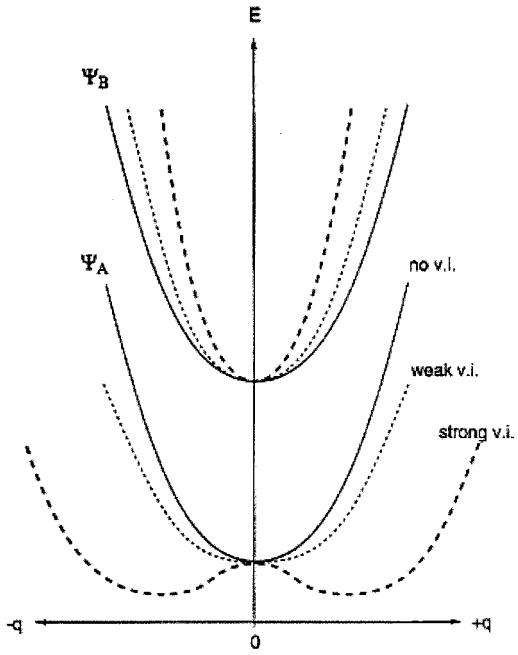

Figure 1. Schematic illustration of the influence of increasing vibronic interaction in a MV system on the ground and excited-state surfaces of a mixed-valence system. Ψ_A and Ψ_A are electronic wave functions for the ground and excited state of the MV system, and q is a normal coordinate for the symmetry-breaking normal mode (in our case: $q = Q_{as}$). For a more detailed description see text.

Methods of Calculations

Vibronic Coupling Model. We introduce here the basics of a simple vibronic coupling model used in this paper and discussed in detail elsewhere.[3] We will start from the more general adiabatic picture and show how the equations may be simplified in a diabatic model.[3]

Consider a molecular system built of two metal centers[11] in two different oxidation states (in our case the oxidation numbers differ always by 1), bridged by an anion − ABA. Constrain this system to a linear symmetric geometry. Such triatomic system exhibits four vibrational modes: a symmetric stretch (ν_s, σ_g), an asymmetric stretch (ν_{as}, σ_u), and a doubly degenerate bending mode (ν_{bend}, π_u). The normal coordinates assigned to these modes are labeled Q_s, Q_{as}, and Q_{bend}, respectively. The problem at hand is to evaluate the nuclear dynamics in the subspace of those coordinates.

The most interesting coordinate to us is the asymmetric stretching one (Q_{as}). According to the model proposed,[3] the eigenvalues of the matrix of the potential energy along Q_{as} normal coordinate (from here termed simply Q) may be approximately expressed as

$$E_{\pm} = {}^1/_2 kQ^2 \pm \sqrt{(\Delta^2 + V^2Q^2)} \qquad (1)$$

where Δ/eV is the electronic coupling parameter, V/eV Å^{-1} is the vibronic coupling constant, and k/eVÅ^{-2} is the force constant for the asymmetric stretch in the hypothetical absence of vibronic coupling. A schematic plot of eq 1 for various extreme cases is presented in Figure 1.

The "±" notation (− is lower state ≡ g, + is upper state ≡ e) refers to the two PES's describing the ground and an excited state of a system. These two states are presumed to be conjugated: their wave functions (Ψ_A and Ψ_B) are constructed from initial wave functions Ψ_1 and Ψ_2 for the two AB subunits from which the system was created.[12] Δ is called the electronic coupling parameter because it is determined by the electronic functions (at $Q_{as} = 0$) and couples them. A basic assumption of the model is that Δ is small compared to the electronic binding energy within the two subunits brought together to form the ABA molecule.[13]

As may be seen in Figure 1, a familiar representation, electronic coupling results in appearance of two sheets of the potential energy surface (PES). They are separated in energy by 2Δ at $Q_{as} = 0$, at zero vibronic coupling. Vibronic coupling results in an even stronger splitting of the two PES sheets (the split increases with Q_{as}). Both resulting sheets of this *adiabatic* potential have an extremum at $Q = 0$, its curvature being

$$k_{\pm}' = k \pm V^2/\Delta \qquad (2)$$

This means that the vibronic coupling increases the curvature of the upper sheet and lowers the curvature of the lower sheet, in comparison with the situation where vibronic coupling is absent. This phenomenon is also known as "softening of the asymmetric mode" (in the ground state) because it leads to an effective decrease in force constant for the asymmetric stretching mode (see Figure 1), while the force constant for symmetric stretch remains practically unaffected. The "softening of the asymmetric mode" will be crucial in our further considerations.

If

$$\Delta < V^2/k \qquad (3)$$

then $k_-' < 0$. In other words, vibronic mixing of different electronic terms (for example Σ_g with Σ_u via a σ_u vibration) leads to the *instability* of the reference (symmetric) nuclear configuration. From this formal similarity to the first-order Jahn−Teller effect, vibronic coupling is sometimes called the pseudo-JT effect or, less correctly, the second-order JT effect.

If eq 3 is true, then the lower PES has the character of a double-minimum well (see Figure 1), with two equivalent energy minima at

$$Q^0{}_{\pm} = \pm \sqrt{>[(V/k)^2 - (\Delta/V)^2]} \qquad (4)$$

and with the curvature k'' at $Q^0{}_{\pm}$ being

$$k'' = k - k^3\Delta^2/V^4 \qquad (5)$$

If condition (3) is fulfilled, the VC is considered to be *strong*, and if the opposite be true, it is considered *weak*. An additional effect arising from vibronic coupling is substantial anharmonicity (called vibronic anharmonicity) of the asymmetric stretching mode. It is known that even the linear vibronic interaction terms which mix different sheets of an adiabatic potential may lead to significant anharmonicity.[14]

When VC is *strong*, there arises a barrier E_{activ} for thermal electron transfer between two nonequivalent centers, given by[3]

$$E_{activ} = {}^1/_2(V^2/k + k\Delta^2/V^2) - \Delta \qquad (6)$$

If E_{activ} is large in comparison with the energy of the asymmetric vibrational mode determined at $Q^0(h\nu''_{as})$, the charges in system are strongly localized (two different oxidation states are "frozen in"). If E_{activ} is small, charge is delocalized between the two metal centers (which are now *equivalent* on a time scale long enough to average them upon vibration).

Having eqs 4−6, one may now derive the respective equations in the diabatic case (i.e., when $\Delta = 0$; both PES's are now two

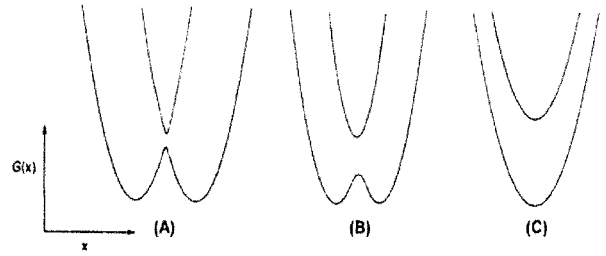

Figure 2. PES's for ABA molecule along the normal coordinate *x* for the asymmetric stretching vibration (a harmonic potential model is used): A) weak electronic coupling, B) medium coupling, C) strong coupling. Values of k and V are kept constant.

crossing parabolas). One easily obtains

$$Q^0{}_{\pm} = \pm(V/k) \tag{7}$$

$$k'' = k \tag{8}$$

$$E_{\text{activ}} = {}^1/_2V^2/k \tag{9}$$

Let us concentrate now on the vibronic coupling element, V − a central parameter of the BCS theory of superconductivity as well.[15] As may be deduced from eq 7,

$$V = k|Q^0{}_{\pm}| \tag{10}$$

i.e., *V* measures directly the difference, in the two oxidation states, of the equilibrium displacement along the antisymmetric normal coordinate. If *V* is large, the localization of charges is strong and the $Me^{n+}-X^-$ bond length differs much from that for $Me^{(n+1)+}-X^-$. Of course, $Q^0{}_{\pm} = 0$ does not imply $V = 0$ in an adiabatic model. This is because in the adiabatic picture the properties of a symmetrical IV system depend strongly on the values of *both* the electronic and vibronic coupling (Δ and *V*).

As shown by eq 3, whether a molecule distorts under the influence of a SOJT effect depends on three factors: the energy separation 2Δ between states A and B (at $Q_{\text{as}} = 0$); the extent to which Ψ_A and Ψ_B interact in lower symmetry (given by the vibronic coupling element *V*); and the size of the quadratic force constant (*k*) for the symmetry-breaking normal mode in the lower electronic state Ψ_A, in the absence of vibronic interaction.

Vibronic interactions *always* occur when an element of symmetry is present, but they may not lead to the energetically favorable distortions if Δ is too large (the effect of increasing Δ with *k* and *V* kept constant is illustrated in Figure 2), *V* is too small, and *k* offers too much resistance to allow a distortion.

In the real world of computational practice, it is not easy to tell whether symmetry breaking is *real* or *artifactual*. In many cases different computational methods lead to results differing qualitatively in their predictions (of an asymmetric or a symmetric structure).[14] In any case, symmetry-breaking mode softening *always* indicates substantial vibronic coupling in the system. We will follow this phenomenon by presenting data for the ratio of computed force constants for asymmetric and symmetric stretching, $G = k_u/k_g$. We want to emphasize that the model presented above uses a *linear off-diagonal coupling constant*. The *V* used in eqs 1−10 is a matrix element denoted often as $h_{eg}(Q_{as})$ and by definition equal to $\langle e|\delta H/\delta Q_{as}|g\rangle$. We do not consider here terms higher than linear, e.g., $\langle e|\delta^2 H/\delta Q_1 \delta Q_2|g\rangle$, describing coupling of e and g electronic states via a $(Q_1 + Q_2)$ overtone.[16] In the first paper in this series we have defined carefully the different kinds of VCCs found in the literature.[17]

QM Computations. In diatomic molecules (studied by us in a previous paper), the simple stretching vibration preserves the symmetry of the wave function throughout the vibration. Thus, vibronic interaction (inherently present also in diatomic molecules) obviously cannot lead to a symmetry-breaking distortion. Hence, it is not easy to determine quantitatively *V* for diatomics. This is why we have chosen open-shell triatomic species as the subject of this study.

Computations of open-shell systems are associated with plenty of troubles. The best methods to compute radicals appear to be density functional theory (DFT) and complete active space SCF (CASSCF) methods with polarization and diffuse functions added in.[14] We have chosen the DFT method (B3LYP), a relatively computationally nondemanding one for small molecules.

However, using DFT we also encountered problems. Among these were density matrix symmetry breaking (with consequent loss of exact degeneracy of the π bending modes), failure of Coulomb series, and many convergence problems. We could not, for example, optimize linear symmetric structures for F_2Cl, F_2Br, F_2I, I_2Cl, K_2F, Rb_2F, Cs_2F, Na_2H, K_2H, and Cs_2H. This is why in some cases we used a PES[18] scan along the symmetric stretching coordinate to determine the approximate geometry at the energy minimum.

In many cases optimization with no symmetry constraint led to bent structures. Calculated imaginary frequencies for bending modes in the linear symmetric structures were an obvious indication of bending. Fully aware of these preferences, we included such molecules, kept linear, in our study in their nonequilibrium geometries. Our focus here is on vibronic coupling along the asymmetric stretching coordinate, because of its strong impact on the IVCT process. This is why we have constrained a linear symmetric arrangement of nuclei.

The AB bond length of ABA systems (assumed to be doublets) was optimized with the DFT/B3LYP method, using Gaussian'94 package.[19] At the same nuclear arrangement we have computed harmonic frequencies. We used a 6-311++G** basis set[20] for light elements and core potentials (LANL2DZ[21]) for K, Rb, Cs, Br, and I. Independently we performed calculations with a UHF method with a 6-31G** basis set. The data presented in this paper derive only from DFT calculations. However, it is important to know that essentially the same *trends* for *G* and k_u are obtained with 6-31G**/UHF computations. The greatest qualitative differencies between DFT and UHF methods resulted when small basis sets (STO-6G, 6-31G) were used (data not presented). We have also observed that in order to obtain geometries of ABA molecules close to those predicted by DFT, it is essential to use as large as possible (in our case 6-311++G**) basis sets, regardless of the method used.

Our main purpose is to evaluate vibronic coupling constants. This may be done in several independent ways.

One may calculate *both* the lower and upper curve in Figure 1. This provides immediately Δ (it is half of energy separation of ground and excited state at $Q_{as} = 0$). Given calculated (analytically or numerically) k_+' and k_-', one may determine *V* (together with k) according to eq 2. However, this method has certain limitations. First, it requires the CIS procedure to determine excited state surfaces (CIS is not available within the DFT framework). Second, radicals usually have many low-lying excited states and it is not easy to guess which excited state should be considered (symmetry considerations may help).

One may calculate exclusively the ground-state PES. Then, there are two cases: the system is asymmetric, or it is symmetric along Q_{as}. In the first case (Q^0 is known) the three equations,

TABLE 1: Values of *k*, *V* and Δ As Found in Best Fits of PES's to Eq 1 for Four Molecules

	Cl_3	Br_3	Br_2Cl	Br_2F
k/au Å^{-2}	0.94 ± 0.03	0.98 ± 0.06	0.60 ± 0.11	1.02 ± 0.03
V/au Å^{-1}	0.34 ± 0.04	0.11 ± 0.06	0.02 ± 0.01	0.21 ± 0.07
Δ/au	0.20 ± 0.02	0.05 ± 0.03	0.03 ± 0.01	0.09 ± 0.03

(2), (4), and (6)[22] allow determination of three parameters: *k*, *V*, and Δ. However, this method fails for a symmetric ground state because there are too few equations to find *k*, *V*, and Δ.

Trying to determine *k*, *V*, and Δ coherently (for both symmetric and asymmetric species) one is left then with fitting procedures. Given a known PES for the ground state one may simply fit *k*, *V*, and Δ in order to satisfy eq 1. Of course, one may also modify eq 1 by using eq 2 with known k_-' (hence, fitting only *V* and Δ).

Initially we chose the fitting method, (iii) to determine the parameters *k*, *V*, and Δ. However, here another problem arises—it appears that *k*, *V*, and Δ are highly correlated with one another. Thus, many sets of *k*, *V*, and Δ satisfy eq 1. This is especially clear for the "symmetric" cases, where reasonable parameters could hardly be found by fitting. To document the troubles we encountered, we show in Table 1 the parameters found for four molecules in the most convincing fits.

It may be seen that relative errors in even these best-fit cases are as high as 30−50% (see errors of *V* and Δ for Br_2Cl and Br_3). Thus, we decided to abandon fitting procedures. Since direct determination of accurate values of *V* in a coherent way for all molecules under study appeared impossible, we approached *V* in another way. As mentioned in a previous section, the "mode softening" phenomenon is intimately connected with vibronic coupling. Significant asymmetric mode softening means strong vibronic coupling (*V* is large). Following up this idea, we have computed the ratio (*G*) of force constants for asymmetric and symmetric stretching in a series of optimized symmetric linear ABA molecules:

$$G = k'_u/k'_g \qquad (11)$$

In the case of vibronic instability we formally assigned a negative sign to the computed imaginary k'_u (hence, *G* is also negative in these cases).

We emphasize here again that our main goal was *not* to determine the correct geometry of *ground state* ABA species. The geometry used by us in calculations of *G* is never a global PES minimum. What we were after was an understanding of *trends* for *G* in certain type of molecules (here: linear symmetric open-shell systems) within a "space of chemical parameters" such as the electronegativity (EN).

Results and Discussion

The plan of this paper is as follows: in section 1 we investigate the $H_2Li^•$ and $H_2F^•$ molecules as instructive examples of ABA species, and as models for "intermediate valence" and "mixed-valence" species, respectively. In section 2 we show computational results for three families of ABA species (A, B = alkali metal, H or halide). We calculate the parameter *G* for a wide range of ABA systems and look for its correlation with difference or sum of electronegativities of A and B elements. In section 3 we will summarize the results obtained, in the process trying to construct some simple rules for maximizing the VCC connected with IVCT process in ABA molecular systems.

1. $H_2Li^•$ and $H_2F^•$ Systems as Simple Examples of ABA Species. In Part 2 of this series (ref 5, section 1) we have looked at the LiH molecule. For heteronuclear AB molecules the $S_0 \rightarrow T_1$ transition often has LMCT character. Thus, the LiH molecule provided us with a simple model to study vibronic coupling for LMCT states. Now we would like to look closer at systems which help to model the VC connected with IVCT states. The simplest molecules exhibiting IVCT are the triatomic ABA• open-shell systems, in particular $Me_2X^•$ ones (Me = alkali metal or H, X = halide). We choose two systems, $H_2Li^•$ and $H_2F^•$, as a starting point for considerations that follow. Using these two ABA• molecules we will emphasize differences between the IV and MV species.

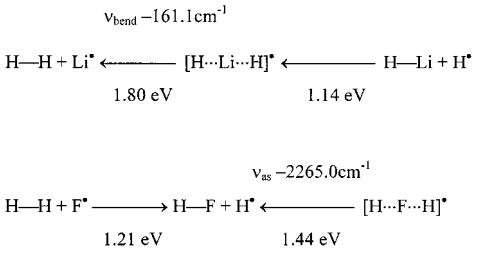

Figure 3. Scheme of the energy minima and saddle points in the linear $H_2Li^•$ and $H_2F^•$ systems, as calculated by the DFT/B3LYP method (with 6-311++*g** basis set). Arrows indicate the way to the lower-energy structure. Numbers over arrows show the frequency for the normal mode (asymmetric stretching, bending) along which the system is unstable. Numbers below arrows indicate the energy difference between two linear structures.

TABLE 2: Optimized Bond Lengths R_0/Å and Force Constants of $H_2Li^•$ and $H_2F^•$ Molecules for Symmetric Linear Geometries Together with Parameter *G* (see text)

	R_0/Å	k_{bend}/mDyne Å^{-1}	k_g/mDyne Å^{-1}	k_u/mDyne Å^{-1}	*G*/1
$H_2Li^•$	1.720	−0.109	0.655	0.554	0.847
$H_2F^•$	1.149	0.067	2.562	−3.354	−1.309

Figure 3 shows the scheme of the energy minima and saddle points in the linear $H_2Li^•$ and $H_2F^•$ systems, as calculated by the DFT/B3LYP method (with 6-311++G* basis set). Table 2 shows the computed force constants of both molecules at their optimized symmetric linear geometries, together with the parameter *G* (see eq 11).

One can observe the following in the Figure 3 and Table 2:

The global energy minimum for the $H_2Li^•$ system corresponds to the IV case (two equivalent H atoms), while the one for the $H_2F^•$ system corresponds to the MV case (nonequivalent H's); these are cases of weak and strong vibronic coupling, respectively;

the linear symmetric structure is thermodynamically unstable for both $H_2Li^•$ and $H_2F^•$; relaxation of symmetric linear $H_2Li^•$ to the lower energy structure occurs via the bending mode, while symmetric linear $H_2F^•$ relaxes along the Q_{as} normal coordinate.

Feature (i) strongly differentiates $H_2Li^•$ from $H_2F^•$. Consider now the vibronic coupling in these two symmetric linear ABA• systems. For $H_2F^•$, a symmetric linear structure is the transition state between two energetically equivalent minima. In other words, the asymmetric stretching mode transforms one asymmetric linear structure to another, chemically identical one.

Using the apparatus of group theory, one may examine vibronic coupling for symmetric linear structures of $H_2Li^•$ and $H_2F^•$. It is *exclusively* the antisymmetric stretching mode σ_u which couples $^2\Sigma_g$ states with $^2\Sigma_u$ ones, and $^2\Pi_g$ with $^2\Pi_u$ ones.[23] The symmetric stretching mode σ_g by symmetry cannot couple these pairs of states. The bending mode (π_u) obviously also does not couple these electronic states. The bending mode does not contribute to distortion of the molecule upon IVCT electronic excitation from one linear structure (one minimum on PES) to

TABLE 3: Computed Molecular Parameters of Optimized Symmetric Linear ABA Molecules: Bond Length (R_0/Å), Force Constant (k_g) and Harmonic Frequency (ν_g) of the Symmetric Stretching Mode, Force Constant (k_u) and Harmonic Frequency (ν_u) of the Asymmetric Stretching Mode and Ratio of Force Constants for Asymmetric and Symmetric Stretches (G)[a]

molecule	R_0/Å	ν_g/cm^{-1}	k_g/mdyne Å^{-1}	ν_u/cm^{-1}	k_u/mdyne Å^{-1}	G/1	molecule	R_0/Å	ν_g/cm^{-1}	k_g/mdyne Å^{-1}	ν_u/cm^{-1}	k_u/mdyne Å^{-1}	G/1
F_3	1.68	363	1.48	679i	−5.16	−3.49	Br_2Cs	3.63	70	0.23	93	0.52	2.25
Cl_3	2.26	279	1.61	226i	−1.05	−0.66	Cs_2Br	3.49	63	0.32	127	0.83	2.61
Br_3	2.67	161	1.20	65i	−0.20	−0.16	I_2Li	2.56	85	0.54	478	0.97	1.78
I_3	3.08	92	0.64	65i	−0.32	−0.49	Li_2I	2.56	352	0.51	316	0.46	0.89
F_2Cl[b]	1.77						I_2Na	2.97	66	0.33	167	0.40	1.23
Cl_2F	2.04	228	1.07	562i	−3.92	−3.68	Na_2I	2.91	172	0.40	169	0.50	1.24
Br_2F	2.09	190	1.68	332i	−1.34	−0.80	I_2K	3.45	57	0.24	141	0.50	2.07
I_2F	2.21	144	1.55	235i	−0.66	−0.42	K_2I	3.35	114	0.30	136	0.58	1.93
Cl_2Br	2.44	261	1.40	94	0.25	0.18	I_2Rb	3.65	54	0.22	97	0.51	2.33
Br_2Cl	2.49	163	1.23	298i	−2.03	−1.65	Rb_2I	3.53	74	0.27	105	0.69	2.53
Cl_2I	2.57	254	1.33	206	1.18	0.89	I_2Cs	3.77	49	0.18	84	0.55	3.05
I_2Cl[b]	2.75						Cs_2I	3.75	56	0.24	93	0.66	2.72
Br_2I	3.37	62	0.18	86i	−0.43	−2.38	H_2Li	1.76	898	0.48	826	0.50	1.05
I_2Br	2.88	102	0.78	68i	−0.24	−0.30	Li_2H	1.57	475	0.93	1886	2.24	2.41
H_2F	1.15	2077	2.56	2265i	−3.35	−1.31	H_2Na	2.01	871	0.45	838	0.45	1.00
F_2H	1.10	644	4.64	1539i	−1.44	−0.31	Na_2H	2.01[b]					
H_2Cl	1.50	1831	1.99	1199i	−0.90	−0.45	H_2K	2.43	708	0.30	708	0.31	1.05
Cl_2H	1.50	350	2.52	1421i	−1.22	−0.48	K_2H	2.46[b]					
H_2Br	1.66	1632	1.58	1107i	−0.75	−0.47	H_2Rb	2.61	680	0.28	681	0.28	1.03
Br_2H	1.66	207	2.00	962i	−0.55	−0.28	Rb_2H	2.65	77	0.29	885	0.47	1.61
H_2I	1.81	1541	1.41	695i	−0.29	−0.26	H_2Cs	2.80	642	0.25	656	0.26	1.06
I_2H	1.85	148	1.63	845i	−0.43	−0.26	Cs_2H	2.89[b]					
H_3	0.93	2056	2.51	736i	−0.32	−0.13	Li_2Na	3.09	178	0.13	188	0.20	1.52
F_2Li	1.74	326	1.19	718	2.36	1.99	Na_2Li	3.07	99	0.13	239	0.26	1.95
Li_2F	1.68	575	1.37	693	2.71	1.99	Li_2K	3.57	149	0.09	150	0.12	1.28
F_2Na	2.07	190	0.79	411	2.12	2.70	K_2Li	3.55	62	0.09	190	0.16	1.81
Na_2F	2.03	284	1.09	495	2.89	2.64	Li_2Rb	3.74	143	0.08	134	0.09	1.01
F_2K	2.41	215	0.52	319	1.52	2.94	Rb_2Li	3.72	41	0.09	182	0.14	1.67
F_2Rb	2.72	196	0.43	211	0.66	1.53	Li_2Cs	4.00	132	0.07	123	0.07	0.96
F_2Cs	2.91	180	0.36	180	0.45	1.23	Cs_2Li	3.98	30	0.07	163	0.11	1.58
Cl_2Li	2.18	191	0.75	567	1.44	1.91	Na_2K	3.72	77	0.08	98	0.17	2.07
Li_2Cl	2.16	438	0.79	460	1.13	1.43	K_2Na	3.72	58	0.08	101	0.15	1.96
Cl_2Na	2.53	156	0.50	286	1.21	2.41	Na_2Rb	3.88	74	0.07	78	0.11	1.50
Na_2Cl	2.52	206	0.58	277	1.29	2.24	Rb_2Na	3.88	38	0.07	90	0.12	1.70
Cl_2K	3.05	126	0.33	187	0.78	2.38	Na_2Cs	4.14	70	0.07	71	0.09	1.32
K_2Cl	2.95	136	0.42	233	1.16	2.73	Cs_2Na	4.14	28	0.06	82	0.10	1.58
Cl_2Rb	3.25	118	0.29	143	0.57	1.99	K_2Rb	4.36	49	0.06	56	0.10	1.78
Rb_2Cl	3.14	85	0.37	197	0.89	2.44	Rb_2K	4.36	33	0.06	63	0.10	1.84
Cl_2Cs	3.49	108	0.24	117	0.38	1.60	K_2Cs	4.61	45	0.05	47	0.07	1.50
Cs_2Cl	3.35	64	0.32	180	0.73	2.25	Cs_2K	4.62	24	0.05	53	0.07	1.56
Br_2Li	2.40	108	0.54	377	0.61	1.13	Rb_2Cs	4.76	29	0.04	36	0.08	2.00
Li_2Br	2.34	395	0.65	377	0.68	1.05	Cs_2Rb	4.76	23	0.04	38	0.08	1.90
Br_2Na	2.69	99	0.45	248	0.92	2.02	Li_3	2.88	196	0.16	298	0.37	2.31
Na_2Br	2.69	193	0.50	212	0.82	1.64	Na_3	3.26	91	0.11	132	0.24	2.11
Br_2K	3.13	78	0.28	171	0.74	2.63	K_3	4.22	49	0.06	71	0.12	2.09
K_2Br	3.10	130	0.39	173	0.92	2.39	Rb_3	4.50	32	0.05	45	0.10	2.06
Br_2Rb	3.30	75	0.26	126	0.77	2.95	Cs_3	5.03	22	0.04	32	0.08	2.03
Rb_2Br	3.28	83	0.35	140	0.93	2.68							

[a] Negative value of k_u and "i" standing after ν_u indicate imaginary frequency. [b] For these molecules we met computational problems, as described in the *Methods of Calculations* section.

the second minimum (also a linear structure) (Figure 2). In some cases, however, the π_u mode may couple effectively a $^2\Sigma_g$ state with a $^2\Pi_u$ one, or a $^2\Sigma_u$ state with a $^2\Pi_g$ one (the former is the case for $H_2F^\bullet$, while the latter is true for $H_2Li^\bullet$). In this paper we do not consider coupling via the bending mode, because this normal mode preserves charge delocalization between two equivalent atoms, and hence the IV character of a system. Only the asymmetric stretch allows charge or electron flow in a molecule, a matter of fundamental interest to us as we look ahead to understanding superconductivity.

As mentioned above, the σ_g mode does not contribute to the vibronic coupling of $^2\Sigma_g$ states with $^2\Sigma_u$ ones at $Q_{as} = 0$. However, its role in the ABA$^\bullet$ system is still prominent. After *slight* symmetry breaking by the σ_u mode, the σ_g mode can couple all resulting $^2\Sigma$ states (within the family of such states) as well as all $^2\Pi$ states. This has severe consequences for the geometry of the ground state of $H_2F^\bullet$: the molecule dissociates to HF and H (along a linear combination of Q_{as} and Q_s).[24]

In the next section we look at vibronic coupling via the σ_u mode in symmetric linear ABA$^\bullet$ molecules.

2. Vibronic Coupling via the σ_u Mode in Symmetric Linear ABA$^\bullet$ Systems. The BAB$^\bullet$, ABA$^\bullet$, and $A_3^\bullet$ molecules (A, B = H, Li, Na, K, Rb, Cs, F, Cl, Br, I) studied here belong to three chemically distinct groups: intermetallics $\{Me^1Me^2_2\}$, "salts" $\{MeX_2$ and $Me_2X\}$, and interhalogens $\{X^1X^2_2\}$. Species containing H, such as MeH_2 and Me_2H, mediate between intermetallic species and "salts". And HX_2 and H_2X are intermediate between "salts" and interhalogen species. Homonuclear $(Me)_3$ and X_3 molecules are also included in the study.

Assuming MV character of the ABA molecules considered, and using the electronegativity as a formal criterion, one might assign formal (integer) oxidation numbers to A atoms. The IVCT assisting a vibronic coupling in species studied by us formally involves $(-1, 0)$ and $(0, +1)$ pairs of oxidation numbers, either common (as Li^{1+} and Li^0 in Li_2F) or more unusual ones (such as I^{1+} in I_2F, or Li^{1-} in Li_2Cs). For a 19th century chemist, these molecules would definitely belong to several different, although fascinating worlds.

Let us take the advantage of modern computational chemistry and examine a spectrum of molecular parameters in one large

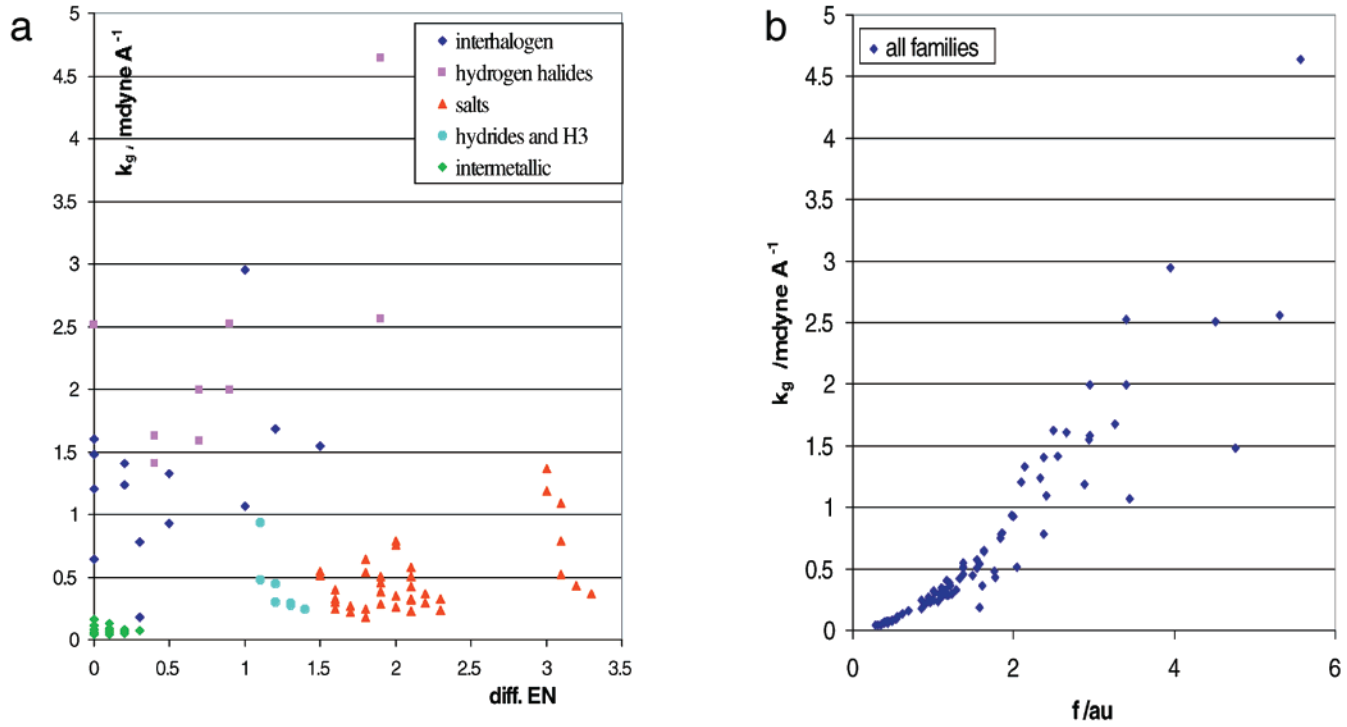

Figure 4. (a) Plot of k_g versus diff.EN for ABA molecules. (b) Plot of k_g versus f for ABA molecules.

family of molecules. Table 3 summarizes values of the force constants for symmetric and asymmetric stretching modes of $Me_2X^{\bullet}$ systems. We show also the value of the AB bond distance as optimized for symmetric linear structures of these molecules, together with parameter G (defined by eq 11).

It is very instructive to plot data from Table 3 versus a "chemical" parameter, for example a difference of Pauling electronegativities for A and B components of an $ABA^{\bullet}$ system (hereafter abbreviated as diff.EN). In addition, previous studies led us to a variable f, defined as the sum of electronegativities of A and B divided by the AB bond length. f helped us to correlate values of diagonal VCC's for intermetallic species Me^1-Me^2, salts MeX, and interhalogen species X^1X^2. Now we want to test utility of f for triatomic systems.[25]

Let us begin with the symmetric force constant, k_g. Parts a and b of Figure 4 show the dependence of k_g on diff.EN and f, respectively.

One can see in Figure 4 that the largest values of k_g are observed for interhalogen species (including hydrogen halides HX_2 and H_2X), followed by salts and hydrides. The smallest values are for intermetallic species. Similar trends have been observed by us previously for E_{exc} and VCC in closed-shell AB molecules.

Figure 4b is of a great importance to us. In Figure 4b values of k_g for interhalogen species, salts, and intermetallic species has been unified in one, almost monotonic dependence on the parameter f. A similar regularity has been previously obtained for the dynamic VCC in closed-shell AB molecules.[5] Hence, both first and second derivatives of the potential energy along certain nuclear normal coordinates in diatomics and triatomics are monotonic functions of one simple semiempirical parameter f. This also means that values of k_g may be now deduced from the periodic table, given known EN's and approximate radii for elements.

Encouraged by such regular behavior of k_g, we want to now examine values of k_u (which is sensitive to vibronic coupling along Q_{as}) in ABA molecules. We plot k'_u versus f in Figure 5.

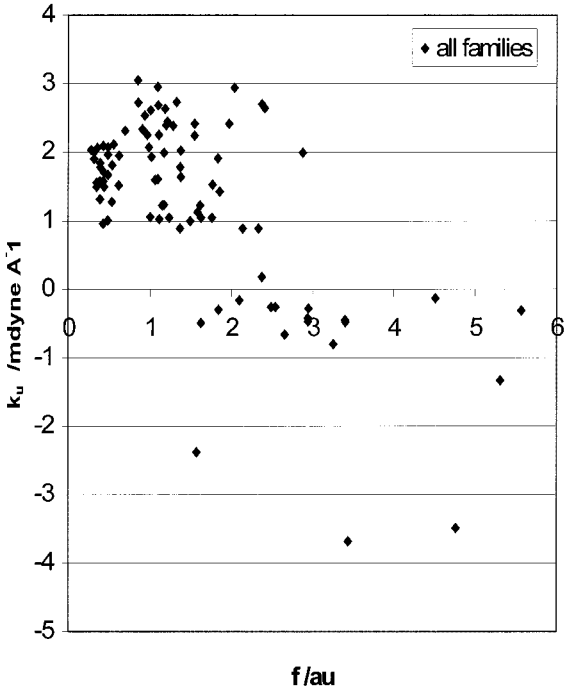

Figure 5. Plot of k'_u versus f for ABA open-shell species.

As may be seen from Figure 5, there does not exist a clear quantitative correlation between the force constant for asymmetric stretching k'_u and the parameter f. One may observe, however, a certain rough correlation, namely that most of points corresponding to negative values of k'_u occur for $f > 2$. There is no point corresponding to negative k'_u for $f < 1.5$. Conversely, there are only few points with $k'_u > 0$ for $f > 2$, while the majority of points with $k'_u > 0$ is for $f < 2$. This indicates that if one wants strongly negative values of k'_u one should provide large value of f.

Our main interest is now in the parameter $G = k'_u/k'_g$. In Figure 6a–c we show the G versus f dependence. We emphasize

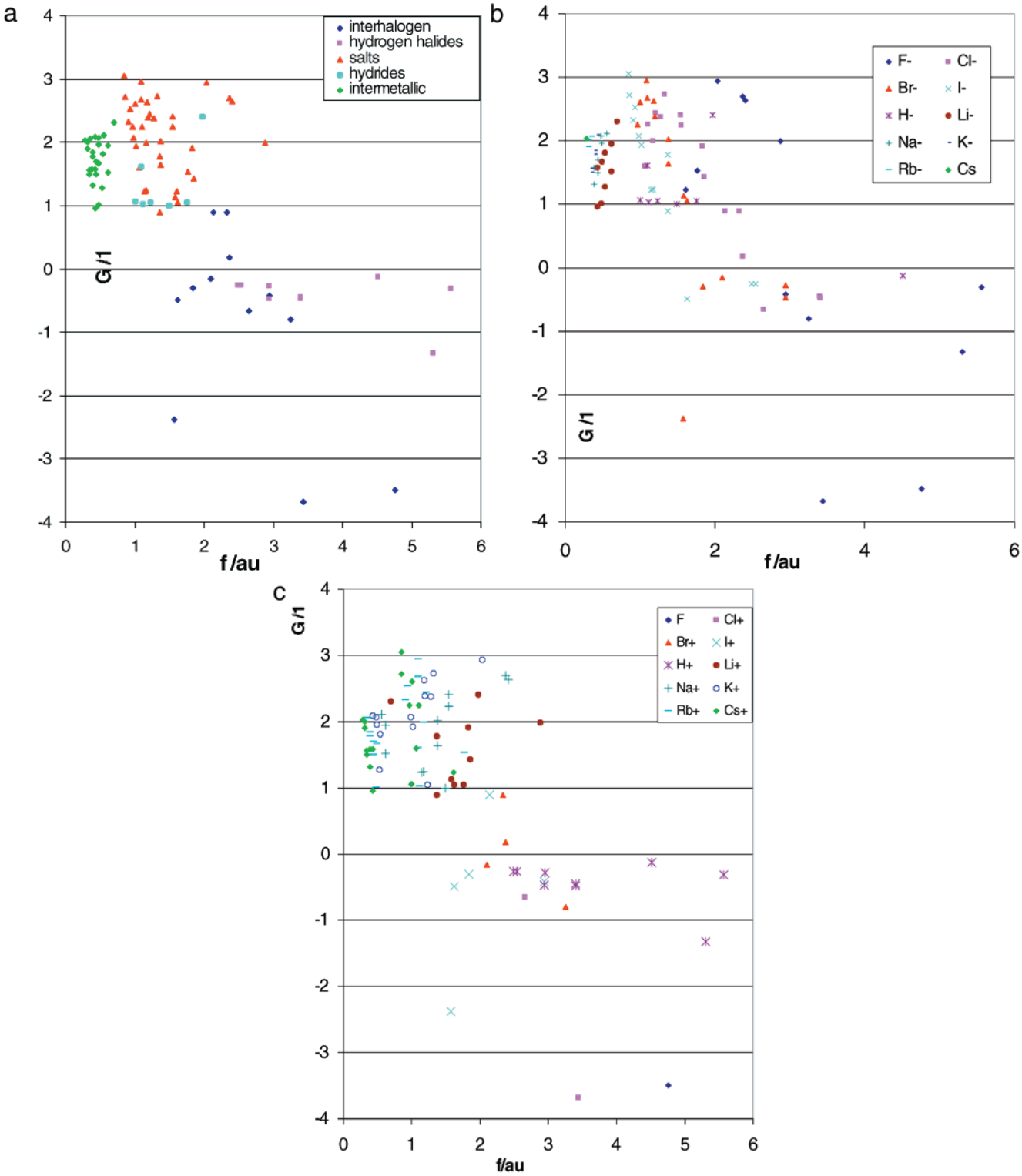

Figure 6. (a) Plot of G vs f for ABA open-shell species. The affiliation of an ABA molecule to a certain family is emphasized. (b) Plot of G vs f for ABA open-shell species. The role of the anion present in a molecule is emphasized. (c) Plot of G vs f for ABA open-shell species. The role of the cation present in a molecule is emphasized.

in these plots the affiliation of a given molecule to a certain family (Figure 6a), or the presence of a certain anion (Figure 6b) or cation (Figure 6c) in a given molecular system.

In may be noticed in Figure 6a that molecules strongly affected by vibronic coupling along the Q_{as} coordinate belong exclusively to the interhalogen species, including hydrogen halides. Conversely, all "salts" (including hydrides) have positive values of G. The largest (most positive) values of G (near +3) are recorded for I_2Cs, Br_2Rb, and F_2K, while the most negative values of G are noted for Cl_2F, F_3, and Br_2I. Interestingly, these observations correspond to our previous findings for diatomics.[5] There we have observed that the largest values of diagonal VCC in closed-shell AB molecules are calculated for interhalogen molecules (F_2, FCl, Cl_2) and for H-containing interhalogen molecules (HF, HCl).

Has G its own "chemistry"? Evidently, groups of points for molecules containing either a certain cation or a certain anion may be distinguished in Figure 6b,c. This is most clear for

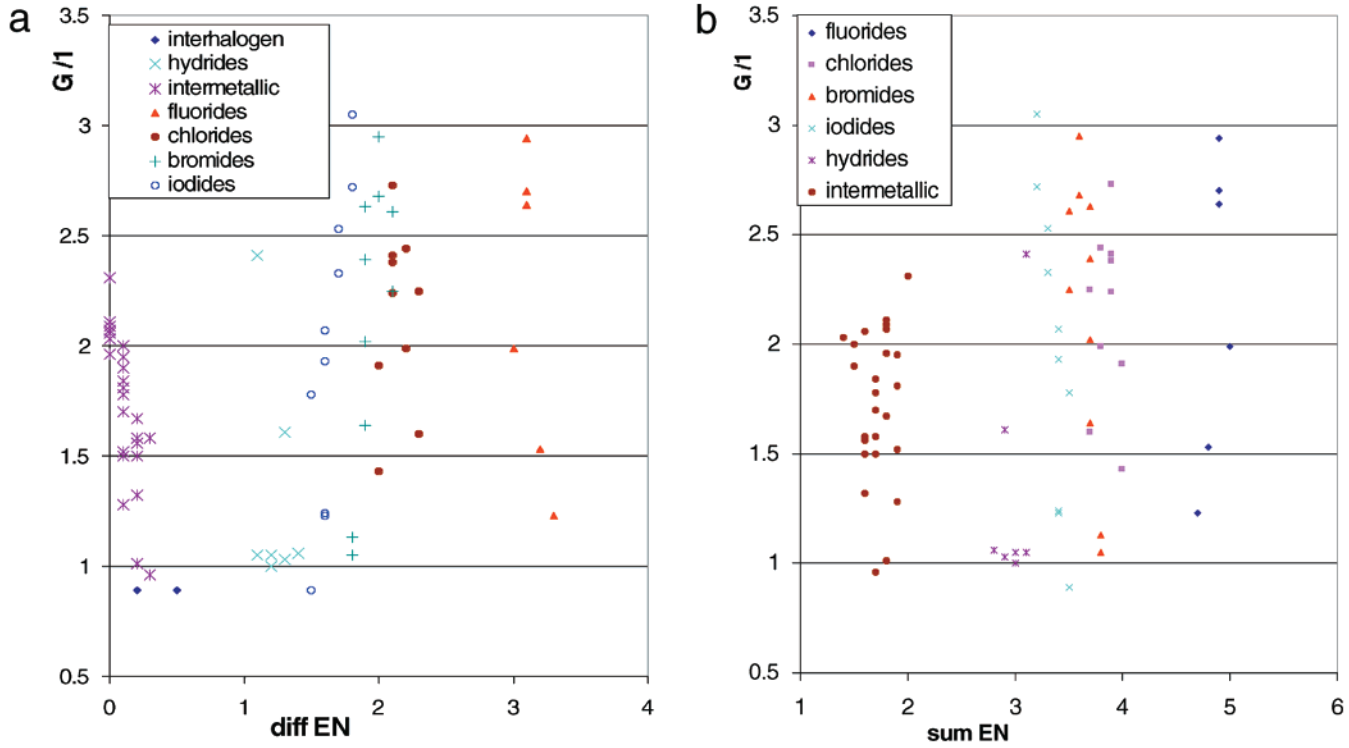

Figure 7. (a) How G varies as a function of the difference of electronegativities of A and B elements (diff.EN) constituting the ABA or BAB molecule. Only points for G > 0.8 are plotted. (b) G vs sum of electronegativities of A and B elements (sum EN) constituting ABA or BAB molecule. Only points for $G > 0.8$ are plotted.

iodides, bromides, chlorides, and "lithides". The same is true for cations: I^+, H^+, Li^+, Na^+, and Cs^+. Points for fluorides fall on a distinct curve, but are more scattered for large f's.

The general trend found within a family containing a given anion is very interesting. Namely, the G vs f dependences for Cl^-, Br^-, and F^- seem to have maxima at certain values of f (f_{opt}). For iodides a monotonic decrease of G vs f is observed, while for "lithides" and "sodides" the opposite is recorded − a monotonic increase of G vs f. In the next paper[26] we will try to rationalize the observed relations within a MO framework.

The observation of a maximum G within certain families containing a given anion is of importance to us. It indicates that for a given anion, there is a paired cation which may provide maximum resistance of a molecular system to a distortion ruled by vibronic coupling. Substituting this cation by another one (leading to f either smaller or larger than f_{opt}) destabilizes the system vibronically.

Surprisingly, it is much more difficult to observe similar regular behavior in Figure 6c, which emphasizes the role of the cation in a triatomic system. For example, (f, G) points for Cs^+-containing species create two branches, both monotonically decreasing with f. Points for other cations exhibit even more complex behavior.

Molecules containing H (either H^+ or H^-) are the greatest surprise to us. In Figure 6b one may see (in contrast to the G vs f regularities observed for other anions) that points for H^- fall on a rather flat curve. Similarly, in Figure 6c the G, f correlation for H^+-containing molecules also seems to be flat.

It is clear that analysis of vibronic coupling in open-shell triatomics is much more complex than analysis of VC in closed-shell diatomics. The computational observations we have so far might possibly be illuminated by correlation of G with other "chemical parameters". Hence, in Figure 7a,b we plotted G as a function of (a) the difference and (b) the sum of EN of A and B elements constituting molecule ABA. In this case we look exclusively at points with $G > 0.8$, which were the least scattered in Figure 6b,c. In other words, we want now to see how one may vibronically destabilize "salts" and intermetallic species, relatively vibronically stable in comparison to interhalogen compounds.

As one can see, the plots presented in Figure 7a,b are quite similar to each other. Moderate vibronic coupling ($G \in$ 0.9−1.2) is achieved in almost all families: intermetallics, hydrides, iodides, bromides, and fluorides. Hence, regardless of the "chemical" identity of a given molecule (salts or intermetallics), a similar degree of vibronic coupling may be reached. This strongly distinguishes the off-diagonal coupling constant in triatomic molecules from the diagonal CC in diatomic ones: the diagonal CC never reached large values in intermetallic species AB.[5] We emphasize that two branches of points in Figure 7b for chlorides and bromides can *not* be assigned to corresponding ABA and BAB (hence (s,p,s,) and (p,s,p)) subfamilies of these species.

3. How To Maximize VCC for Q_{as} in $Me_2X^\bullet$ Systems—Summary. The analysis of the computational results in the previous section left us with many uncertainties and questions. Triatomic open-shell species are much more complex, from the point of view of vibronic coupling, than closed-shell diatomics.

It seems advisable to introduce here a notation for triatomics similar to one we introduced for diatomics:[5] we will speak of (p,p,p), (p,s,p), (s,p,s), and (s,s,s) families of triatomics, depending on the block of the periodic table to which the A and B elements of A−B−A molecule belong. There are the generalizations that emerge for all (p,p,p), (p,s,p), (s,p,s), and (s,s,s) families of triatomic molecules:

(i) The smallest (large negative) values of G are computed for interhalogen compounds, including hydrogen halides. The (p,p,p) molecules usually exhibit "strong vibronic coupling", leading to appearance of asymmetric linear structures as distinct minima in the PES along Q_{as}. Small compact hydrogen is the

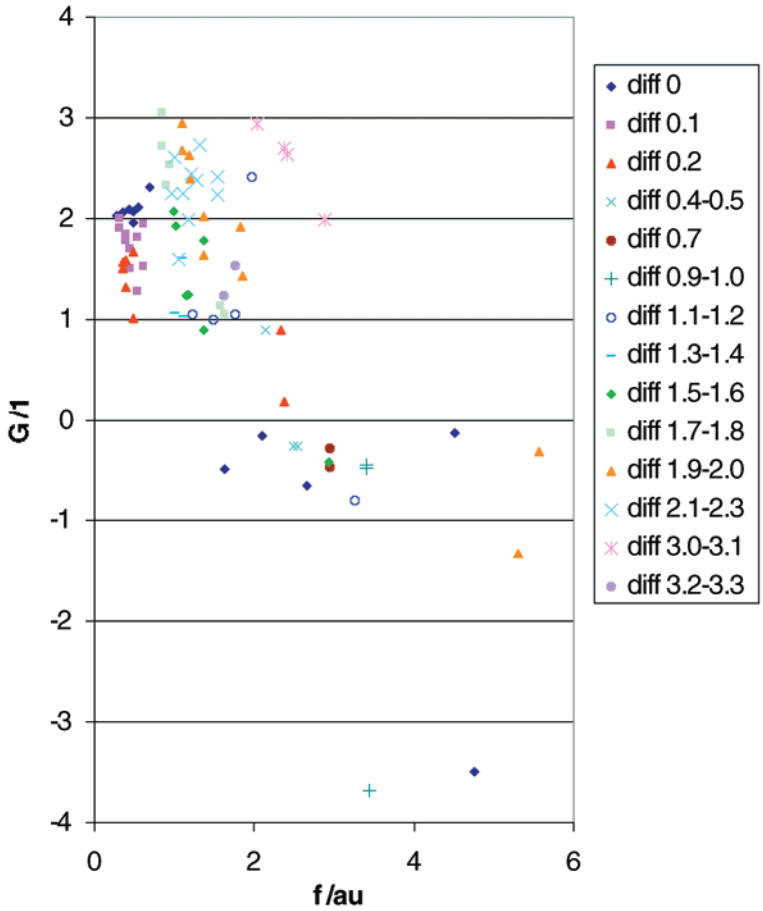

Figure 8. Values of *G* for families of ABA molecules with the same difference of electronegativity between B and A elements ("diff" in legend to the Figure).

only s-block element which can effectively compete with p-block elements in reaching large negative values of *G*. Thus, H-based (p,s,p) and (s,p,s) systems are also strongly vibronically unstable. There is a temptation here to associate the observation with hypervalence, the specifics of bonding in these molecules. But these molecules are radicals and not classical closed shell systems of the XeF_2 type.

(ii) All intermetallic molecules are vibronically stable. However, in a few cases some asymmetric mode softening may be noted, as for: Li_2Rb ($G = 1.01$), Li_2K ($G = 1.28$), and Na_2Cs ($G = 1.32$).

(iii) Most salt-like molecules are relatively vibronically stable. For instance, systems such as F_2Na and Na_2F, with diff.EN $= \pm 3.1$, are very stable along Q_{as} ($G \approx 2.7$).

(iv) Most molecules with large *f* values have a negative value of *G*.

(v) Negative values of *G* may be obtained for ABA molecule with various differences of electronegativities between A and B elements (see Figure 8). Vibronically unstable species occur for a wide range of diff.EN $\in 0-2$.

The above observations might be useful for designing molecules with large negative values of *G*. The *G* vs *f* relationship (iv) is of the greatest significance, because it constrains most severely the "space" of molecules with strong vibronic instability.

For visualization of trends described above we have constructed a 3D view of the vibronic stability parameter *G* in the periodic table (Figure 9). The ordinates used to generate this graph are the sum and difference of EN between B and A elements in an ABA molecule.

We note an interesting symmetry between *G* values for ABA and BAB molecules (with opposite values of diff.EN). This is especially clear for salts and intermetallics. Also, one might expect existence of a boundary zone (at $G \approx 0$) between positive (for salts, intermetallics) and negative (for interhalogens) values of *G*. Where is this boundary zone? We will answer this question in next paper,[26] where we construct maps of the vibronic stability parameter *G*, and we search for MO explanations of the trends reported here.

Conclusions

We have performed electronic and vibrational structure calculations for a large set of ABA molecules at their optimized symmetric linear geometry (which may or may not be the equilibrium geometry). The focus has been on *G*, defined as the ratio of force constants for the antisymmetric and symmetric stretching mode. *G* is a sensitive indicator of vibronic coupling along Q_{as} in a molecular system. We have observed that *G* usually has positive values for intermetallic and salt-like molecules, while *G* is usually negative for interhalogen compounds and hydrogen halides. We tried to correlate *G* with the difference and sum of electronegativities of B and A elements as well as with parameter *f*. The latter parameter (found to be useful in previous work) is defined as the sum of A and B electronegativities divided by AB bond length. It appears that *f* has substantial diagnostic value in a search for large negative values of *G* (i.e., molecules with high vibronic instability and large values of the vibronic coupling constant). The parameter *f* also appears to be of more general analytical and predictive

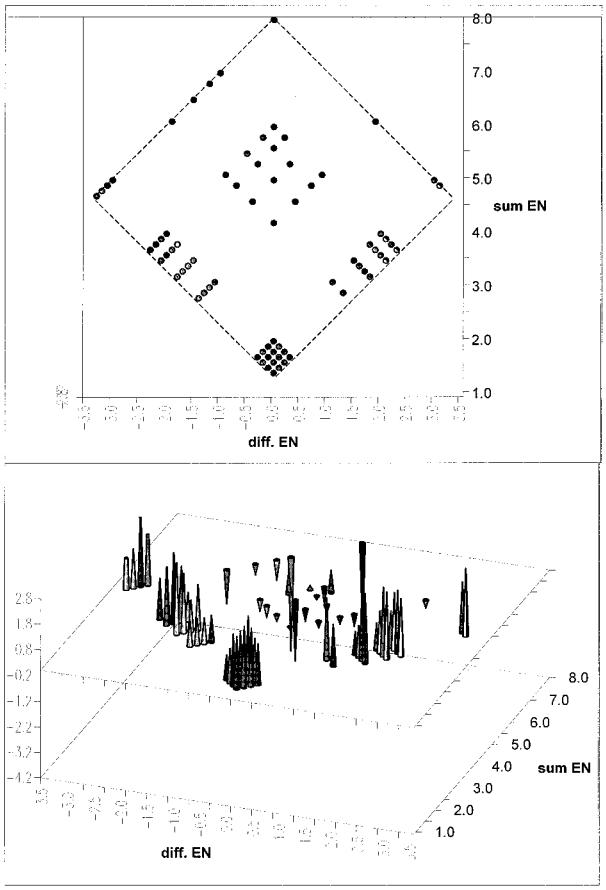

Figure 9. 3D plot of parameter *G* for ABA molecules versus the difference and sum of electronegativities of B and A elements (bottom) together with its projection on a diff.EN/sum EN surface (top). The dotted line marks the available "space" of chemical elements.

utility—interestingly, it correlates also with the force constant for the symmetric stretching mode.

Acknowledgment. This research was conducted using the resources of the Cornell Theory Center, which receives funding from Cornell University, New York State, the National Center for Research Resources at the National Institutes of Health, the National Science Foundation, the Defense Department Modernization Program, the United States Department of Agriculture, and corporate partners. This work was supported by the Cornell Center for Materials Research (CCMR), a Materials Research Science and Engineering Center of the National Science Foundation (DMR-9632275). W. Grochala thanks also to Kosciuszko Foundation for financial support.

References and Notes

(1) The off-diagonal VCC is usually denoted as *V* or h_{eg}. For definition of *V*, see Methods of Calculations.

(2) Creutz, C.; Taube, H. *J. Am. Chem. Soc.* **1969**, *91*, 3988.

(3) See excellent reviews: (a) Bersuker, I. B.; Polinger, V. Z. *Vibronic Interactions in Molecules and Crystals*; Springer-Verlag: Berlin, 1989. (b) Wong, K. Y.; Schatz, P. N. A Dynamic Model for Mixed-Valence Compounds. *Progress in Inorganic Chemistry*; Lippard, S. J., Ed.; John Wiley and Sons: New York, 1981; Vol. 28, p 369. (c) Bersuker, I. B.; *The Jahn−Teller Effect and Vibronic Interactions in Modern Chemistry*; Plenum Press: New York, 1984. (d) Bersuker, I. B. *Electronic structure and properties of transition metal compounds: introduction to the theory*; J. Wiley and Sons: New York, 1996.

(4) Burdett, J. K. *Inorg. Chem.* **1993**, *32*, 3915.

(5) Grochala, W.; Hoffmann, R. submitted to *New J. Chem.* (No2).

(6) Bardeen, J.; Cooper, L. N.; Schrieffer, J. R. *Phys. Rev.* **1957**, *108*, 175.

(7) Gutsev, G. I.; Boldyrev, A. I. *Chem. Phys. Lett.* **1982**, *92*, 262.

(8) Rehm, E.; Boldyrev, A. I.; von, R. Schleyer, P. *Inorg. Chem.* **1992**, *31*, 4834.

(9) Gutsev, G. I.; Boldyrev, A. I. *Chem. Phys.* **1981**, *56*, 277.

(10) Wang, X.; Ding, C.; Wang, L.; Boldyrev, A.; Simons, J. *J. Chem. Phys.* **1999**, *110*, 4763.

(11) In the case of interhalogen species these are also halogen centers.

(12) In the case when an anion *bridges* two metal centers with different oxidation numbers (three atoms) this construction is more complicated than in the case of two interacting $A^{n+}B^{m-}$, $A^{(n+1)+}B^{m-}$ subunits (four atoms).

(13) If this is not the case, it is necessary to include additional terms corresponding to low-lying excited states; the first-order perturbation treatment used to obtain eq 1 is inadequate.

(14) Bally, T.; Borden, W. T. Calculations on Open-Shell Molecules: A Beginner's Guide. *Rev. Comput. Chem. Vol. 13*; Lipkowitz, K. B.; Boyd, D. B., Eds.; John Wiley and Sons: New York, 1999; p 1.

(15) More precisely, *V* used in BCS describes coupling via *phonons* in the solid state and not via normal modes of *molecular* systems.

(16) For more detailed description of different types of coupling constants see ref 3.

(17) Grochala, W.; Hoffmann, R. submitted to *Chem. Phys.* (No. 1).

(18) A probing step was 0.025 Å.

(19) Gaussian 94, Revision D.3, Frisch, M. J.; Trucks, G. W.; Schlegel, H. B.; Gill, P. M. W.; Johnson, B. G.; Robb, M. A.; Cheeseman, J. R.; Keith, T.; Petersson, G. A.; Montgomery, J. A.; Raghavachari, K.; Al-Laham, M. A.; Zakrzewski, V. G.; Ortiz, J. V.; Foresman, J. B.; Cioslowski, J.; Stefanov, B. B.; Nanayakkara, A.; Challacombe, M.; Peng, C. Y.; Ayala, P. Y.; Chen, W.; Wong, M. W.; Andres, J. L.; Replogle, E. S.; Gomperts, R.; Martin, R. L.; Fox, D. J.; Binkley, J. S.; Defrees, D. J.; Baker, J.; Stewart, J. P.; Head-Gordon, M.; Gonzalez, C.; Pople, J. A. Gaussian, Inc., Pittsburgh, PA, 1995.

(20) (a) Krishnan, R.; Binkley, J. S.; Seeger, R.; Pople, J. A. *J. Chem. Phys.* **1980**, *72*, 650. (b) Clark, T.; Chandrasekhar, J.; von, R. Schleyer, P. *J. Comput. Chem.* **1983**, *4*, 294.

(21) Dunning, T. H., Jr.; Hay, P. J. In *Methods of Electronic Structure, Theory, Vol. 2*, Schaefer, H. F.; III, Ed.; Plenum Press: 1977.

(22) We have observed that using eq 9 instead of eq 6 (i.e., setting $\Delta = 0$) may lead to very different values of *k* and *V* than in an adiabatic picture. Hence, the assumption of diabacity is essentially not valid if one wants to treat all molecules coherently.

(23) If in a complex molecule there are more modes of a given symmetry which can couple two given states, a total dynamic VCC is usually calculated. It is defined as sum of VCC's: $VCC_{total} = \Sigma_i\{VCC_i\}$.

(24) Hence, the two equivalent minima appearing in PES for $H_2F^{\bullet}$ system along Q_{as} (see Figure 3) are not physical. We take these "unreal" structures as *models* for studying the VCC for IVCT process, regardless of the their thermodynamic instability.

(25) It is possible to define *f* in the same way as for diatomics, because ABA molecules contain atoms of two and not three different types.

(26) Grochala, W.; Hoffmann, R. *J. Amer. Chem. Soc.*, submitted.